Hunting alters viral transmission and evolution in a large carnivore

Authors: Nicholas M. Fountain-Jones[1, 2*], Simona Kraberger[3], Roderick Gagne[3], Marie L.J. Gilbertson[1], Daryl R. Trumbo[4], Michael Charleston[2], Patricia Salerno[4,5], W. Chris Funk[4], Kevin Crooks[6], Kenneth Logan[7], Mathew Alldredge[8], Simon Dellicour[9,10], Guy Baele[10], Xavier Didelot[11], Sue VandeWoude[3], Scott Carver[2], and Meggan E. Craft[1,12]

Affiliations:

[1] Department of Veterinary Population Medicine, University of Minnesota, St Paul, Minnesota 55108.

[2] School of Natural Sciences, University of Tasmania, Hobart Australia 7001.

[3] Department of Microbiology, Immunology, and Pathology, Colorado State University, Fort Collins, CO 80523.

[4] Department of Biology, Graduate Degree Program in Ecology, Colorado State University, Fort Collins, CO 80523.

[5] Universidad Regional Amazónica IKIAM, Km 7 Vía Muyuna, Napo, Ecuador

[6]Department of Fish, Wildlife, and Conservation Biology, Colorado State University, Fort Collins, CO 80523.

[7] Colorado Parks and Wildlife, Montrose, CO 81401 USA.

[8] Colorado Parks and Wildlife, Fort Collins, CO 80526 USA.

[9] Spatial Epidemiology Lab (SpELL), Université Libre de Bruxelles, CP160/12 50, av. FD Roosevelt, 1050 Bruxelles, Belgium.

[10] Department of Microbiology, Immunology and Transplantation, Rega Institute, KU Leuven, Herestraat 49, 3000 Leuven, Belgium.

[11] School of Life Sciences and Department of Statistics, University of Warwick, Coventry, CV47AL, United Kingdom.

[12] Department of Ecology, Evolution and Behavior, University of Minnesota, St Paul, Minnesota, 55108

*Nick.FountainJones@utas.edu.au

Key words: Feline immunodeficiency virus, Mountain lion, Selection, Perturbation effect, Phylogenetic diversity, Puma, *Puma concolor*

Authorship statement: NFJ conducted the analysis and wrote the initial draft of the paper to which all authors contributed. KL and MA studied the puma populations in the field and provided the blood samples. SK, DT, PS, RG and SV collected virus and host genetic data. SD, GB, MC and XD contributed to the phylogenetic and transmission tree analyses. MG contributed to the spatial analysis. MEC, SV, KC, CF and SC conceived of the project.

Abstract:

Hunting can fundamentally alter wildlife population dynamics, but the consequences of hunting on pathogen transmission and evolution remain poorly understood. Here we present a study that leverages a unique landscape-scale quasiexperiment coupled with pathogen transmission tracing, network simulation, and phylodynamics to provide insights into how hunting shapes viral dynamics in puma (*Puma concolor*). We show that removing hunting pressure enhances the role of males in transmission, increases the viral population growth rate, and increases the role of evolutionary forces on the pathogen compared to when hunting was reinstated. Changes in transmission observed with the removal of hunting could be linked to short term social changes while the male puma population increased. These findings are supported through comparison with a region with stable hunting management over the same time period. This study shows that routine wildlife management can have impacts on pathogen transmission and evolution not previously considered.

Main:

Human actions commonly alter wildlife populations. A classic example of an alteration is hunting, which often has density and demographic effects on a population [1–4]. Recreational quota-based hunting of carnivore populations is common across the globe [e.g., 5,6], however, the consequences of these actions on pathogen transmission and evolution are largely unknown, and the few available studies report contradictory findings. Theory predicts that for pathogens with density-dependent transmission, hunting-induced decreases in density should decrease transmission rates yet make little difference to transmission dynamics for frequency-dependent pathogens. In practice, empirical data and models suggest that reducing host density can either decrease [7,8] or even increase pathogen transmission and prevalence [9,10]. The complex interplay between host density, demography, and behavior also makes predicting the impacts of hunting on pathogen dynamics complex. Human harvest of wild populations is often non-random (e.g., a preference for large males [1] or a particular behaviour [11]) and if different sexes, ages, or behavioral types contribute disproportionately to disease transmission, this could have implications for disease dynamic[12]. Empirical work shows that population reduction can increase pathogen prevalence via social perturbation [13–17]. For example, culling-induced changes or 'perturbations' to badger (*Meles meles*) territorial behavior was considered a driver of increased bovine tuberculosis transmission among badgers [e.g., 13,17,18]. Culling male badgers may be particularly important, as male-male contact networks are structured over larger spatial scales that potentially facilitate between-group spread of bovine tuberculosis [17,18] However, there is also evidence that population reduction has little impact on canine rabies [19] or Tasmanian devil facial tumor disease [20] dynamics. Recent advances in high-resolution pathogen sequencing and analytic approaches can now elucidate patterns of pathogen transmission and evolution [21–23] that were

previously out of reach. Here we address the effects of hunting on pathogen dynamics by capitalizing on pathogen sequences collected from a detailed study on the demographic effects of hunting [24] as well as from sequences obtained over the same time period in a region where little hunting occurred. Our approach enables us to provide insights into the cascading consequences of hunting, and the cessation of hunting, on host-pathogen dynamics.

RNA viruses are ideal agents for examining the effect of hunting and the cessation of hunting on pathogen transmission and evolution. Genomic variation rapidly accrues in RNA viruses, enabling estimation of fine-scale epidemiological processes (such as transmission between hosts) and the **basic reproduction number (R_0)** [22,25] (see Box 1 for definitions of key terminology highlighted in bold). Altered transmission dynamics and the arrival of new lineages can imprint distinctive evolutionary signatures on RNA viruses as they adapt quickly to changes in host populations they encounter [26,27]. For example, if a change of management that increases contact rates led to a higher frequency of transmission events, the **transmission bottlenec**k may lead to high **purifying selection** since within-host mutations are lost with transmission (e.g., [28]). Conversely, if new mutations entering the host population, for example, via increased host immigration, allow the pathogen to escape immune detection, we may expect an increase in **diversifying selection**. Altered transmission dynamics and new lineages will also shape the phylogenetic diversity of the pathogen [29]. For example, if novel pathogen lineages are frequently arriving into a host population with limited transmission, we would expect to see a pattern of phylogenetic dispersion (i.e., higher phylogenetic diversity than expected by chance [30]). In contrast, phylogenetic clustering (i.e., lower phylogenetic diversity than expected by chance [30]) may be a marker of increased transmission events within a population.

Here we leverage cross-sectional viral data collected from closely monitored puma (*Puma concolor*) in two areas in Colorado during the same time period: a 'treatment region' in which hunting pressure changed over time and a 'stable management region' acting as a control (hereafter 'stable region'). We sequenced viral genes sampled from captured puma for an endemic RNA retrovirus, puma feline immunodeficiency virus (FIV_{pco}), which is a host-specific pathogen considered relatively benign and not associated with overt disease outcomes [31]. FIV_{pco} is a lifelong infection that is not eliminated by sterilizing immunity [32]. Even though FIV_{pco} is endemic in puma populations, novel infections can spread in susceptible and previously infected individuals [33]. As apex predators, puma occur in low density and contact between adults (and potential transmission events) occurs mainly via mating or during territorial fights among males (although contact around food resources may be more common than previously thought [35]). After becoming independent from their mothers at between 10-20 months of age, males nearly always leave their natal range whereas 50-80% of female offspring set up adjoining home ranges [36]. Evidence suggests FIV_{pco} is often transmitted via aggressive interactions, although vertical transmission is also possible [31,34].

We analyzed these viral data using a **transmission network** approach [22,29] that incorporates a stochastic epidemiological model with pathogen genomic data to trace transmission between individual puma. When combined with field observations and host genomic data, this approach enabled us to quantify differences in transmission networks associated with hunting and characterize putative transmission events. The types of aggressive interactions which are transmission relevant are largely unknown (but see [38,39]), but based on our understanding of

puma behaviour [40] we hypothesize the following: 1. A dominance of male to male or female to female transmission should indicate that competition for mates or resources or mates is important. 2. A preponderance of transmission events between related males and females may be indicative of familial transmission and/or vertical transmission. 3. Transmission primarily occurring between unrelated males and females may indicate interactions associated with mating may be important.

We constructed FIV_{pco} transmission networks in both study regions. The treatment region consisted of puma in a ~12000km^2 area in western Colorado in which hunting prior to our study was common practice (see [24]). Hunting was excluded for a five-year period (November 2004 - November 2009, "no-hunting period") and reinstated for a further five years afterwards (November 2009- March 2014, "hunting period"). The harvest rate averaged 15% of the independent puma that used the study area across this five year hunting period, with males favoured by hunters (32 of the 46 pumas harvested were adult males [24]). Hunting was excluded in this region to facilitate a study on the population level effects of regulated hunting on puma in Colorado [24]. During the no-hunting period in the treatment region, the population of independent pumas (i.e., adults and sub-adults) increased from an estimated 23 (2005) to 57 (2009) individuals, with much of this growth occurring between 2007-2010 [24] (i.e., after a two year lag 2005-6, hereafter 'Lag 1'). Adult and sub-adult male survival was significantly higher in the no-hunting period [24] and we hypothesized that this may increase transmission events associated with competition for mates. When hunting resumed November 2009, the overall population declined after a lag of two years with male abundance estimates similar to the start of the no-hunting period (2009-2011, hereafter 'Lag 2', Table S1). However, the decline in abundance of males

144 was severe and rapid with males > 6 years old apparently eliminated from the population after
145 two hunting seasons (mortality rates from other sources such as vehicle strike in both periods
146 were similar [24]). See Tables S1/S2 for a summary of abundance and FIV_{pco} data. In contrast, over
147 the same 10-year period, the stable region in the Front Range of Colorado experienced continued
148 minimal hunting pressures (three individuals harvested from 2007- 2013 [41]) and no change in
149 management practice. Previous genetic analysis revealed that the puma in these regions were
150 genetically distinct with few clear migrants [42]. Nearly all the individuals sampled in both regions
151 were adults and both sexes were evenly represented. Individual survival probabilities in the
152 stable region were unaltered across years [41]. By comparing the treatment and stable regions, we
153 were able to test how demographic changes, including heterogeneity in survival between the
154 sexes, caused by hunting cessation and reinstatement perturb viral transmission networks,
155 epidemiological parameters (e.g., R_0), and pathogen diversity and evolution. In doing so we
156 begin to untangle the complex interplay between wildlife management and pathogen
157 transmission, which is crucial for pathogen-orientated conservation and disease management
158 strategies.

159

160 **Cessation of hunting shifts transmission networks and increases R_0**

161

162 We found that reducing hunting mortality had major effects on FIV_{pco} transmission dynamics.
163 Even though the regions were of comparable geographic size and contained similar puma
164 abundance (Table S2), our estimates of R_0 for the same virus over the 10-year period were two-
165 fold higher in the treatment region compared to the stable region (with non-overlapping 95%

high probability density intervals indicating that the difference is significant, Fig. 1; see Table S3 for sensitivity analysis results). Other model parameters, such as generation time (the time between initial FIV_{pco} infection and onward transmission, Fig. S2), and the proportion of missing cases (Fig. S3), yielded similar estimates in both regions. The burst of transmission in the treatment population after the cessation of hunting (Fig. 1a right panel) was likely a result of transmission between males as they were dominant in the network. In the treatment population, males had an overall mean **weighted degree** (Box 1) double that of females (0.23 compared to 0.08). Only one putative transmission event occurred between sexes, and we detected no female-female transmission events in the treatment region. When we assessed **weighted degree homophily** of male-male transmission events, simulations revealed that the dominance of male-male transmission events in the network was not random (1000 simulated annealing network iterations, $p < 0.001$, Fig. S4a, Table S3). Putative transmission events largely occurred when hunting mortality was eliminated (Fig. 1a), during which time the survival of adults and subadult males was high, average age increased, and the abundance of independent pumas increased [24]. During the hunting period, male survival rates were lower than for either sex in the stable region [24]. Female survival was also reduced in the hunting period but the decline was not as dramatic as it was for males [24]. Females were, however, much less connected in the transmission network in the treatment region compared to the stable region, where they were more connected (Fig. 1b). In contrast to the treatment region, the stable region showed evidence of transmission from females to both females and males. Average weighted degree was higher overall for males than females in the stable region (0.46 vs 0.29). Even though weighted female-female degree homophily was higher in the stable region (0 vs 0.05), our simulations show that we could not reject the null hypothesis that this difference was by chance ($p= 0.692$, Fig. S4b, Table S3). Female-to-female

transmission events in the stable region occurred between highly related females, supporting previous findings of the importance of host relatedness in FIV_{pco} spread for puma in this region [39]. Taken together, our results indicate that lower hunting mortality was associated with an increase in the number of transmission events which were dominated by males.

After hunting was prohibited, the greater survival and increasing abundance of males likely resulted in greater competition between males for mates. As the dominant transmission mode for FIV_{pco} is considered to be via aggressive contacts [43], increased male competition for mates appears a probable explanation for the differences in transmission dynamics. Further interrogation of our transmission network supports this theory, as in all but two instances, male-to-male transmission occurred between individuals with overlapping territories in the treatment region (Fig. 2/S5/S6; based on our radiotelemetry location data (unpublished data, K. Logan). One transmission pair was unusual in having less spatial proximity, yet one puma of this pair was a likely immigrant to the region (M133) and could have passed through M73's territory at some point (Fig. 2). With the exception of M73 (~6 y.o. at time of infection), all individuals involved in these transmission events were between 1-3 y.o., which is a period when males are establishing territories and are starting to compete for access to females [40,44]. Our results suggest it is unlikely that these males transmitted to each other prior to dispersal or via maternal or paternal contacts—since these individuals were not related based on genomic data [45]. While our estimates suggest that we were able to sample approximately 40% of the FIV_{pco} infections in both regions (Table S1, Fig. S3)—arguably good coverage for secretive, free-ranging wildlife—our models account for this type of missing data [22]. For example, nearly all putative transmission events we identified from our transmission networks were between individuals on the landscape at the same time and in most cases were captured in close spatial proximity to each other. The

biological plausibility of these transmission events demonstrates the power of adapting transmission network models to trace transmission and gain epidemiological insights in systems that are difficult to observe.

Hunting alters diversity and selective pressure on the virus

Altered transmission dynamics at a population level were associated with changes in viral evolution and diversity in the treatment region. The increased number of transmission events in the no-hunting period compared to the hunting period was supported by the strong phylogenetic clustering (isolates with less phylogenetic diversity than expected by chance) detected relative to the hunting period (Fig. 3a). While not directly quantified here, differences in intra-host evolutionary rates are unlikely to explain regional differences in phylogenetic diversity as FIV intra-individual evolution rates have been found to be stable across hosts and are roughly equivalent to FIV inter-individual rates [46]. This supports the demographic changes associated with hunting, rather than intra-individual variation, are likely to shape the viral phylogenetic patterns observed. The link between reduced hunting pressure and increased transmission events was further supported as we did not find similar phylogenetic clustering in the stable region or hunting period (Fig. 3a). Moreover, we found little evidence for new lineages arriving during the no-hunting period in the treatment region (Fig. 1a). We further interrogated viral diversity patterns across time using ***skygrowth*** **demographic analyses** [47]. Viral genetic diversity rapidly accrued at the end of the no-hunting period (~2009/2010) before markedly declining after ~2011 when hunting was reinstated (Fig. 3b), closely mirroring male population size estimates (R^2 = 0.8, p = 0.010, Fig. 3c). In contrast, female population size was not significantly correlated to viral population growth rate (R^2 = 0.190, p = 0.630, Fig. 3d). Collectively, the relationships

between host abundance estimates and viral population growth rates support a greater role of male interactions in transmission dynamics across hunting intensities, relative to females. While we lack behavioral observations of puma across time, it is possible that the increase in male density with the cessation of hunting allowed for increased competition for mates and thus aggressive interactions [44]. No such increase in FIV_{pco} diversity and growth rate was detected in the stable population (Fig. S7b/c).

Within the treatment region, the increase in viral diversity was underpinned by greater effects of both purifying and diversifying selection acting on viruses that infected individuals during the no-hunting period compared to the hunting period ($p = 0.01$, likelihood ratio = 6.31). Purifying selection, potentially as a signature of rapid transmission events (e.g., [22]), was dominant in both periods (97.25% sites $\omega < 1$), as is often the case in error-prone RNA viruses, but stronger in the non-hunting period ($\omega_{2\,nh} = 0$, $\omega_{2h} = 0.1$). In contrast, there was no shift in evolutionary pressure in the same periods in the stable population ($p = 0.5$, likelihood ratio = 0.43). While impacting a smaller proportion of the loci overall (2.79% loci $\omega > 1$), there was strong diversifying selection in the no-hunting period as well ($\omega_{3\,nh} = 21.46$, $\omega_{3h} = 2.8$). Using the MEME routine (Mixed Effects Model of Evolution) that tests for selection at individual sites on a proportion of branches [48], we identified five FIV_{pco} loci under diversifying selection in both regions (cutoff: $p \leq 0.1$). Two of sites had non-synonymous substitutions just in isolates in males and, based on our transmission models, the males were likely infected by FIV_{pco} in the no-hunting period. There was no signature of diversifying or purifying selection in the envelope gene (*env*), which was surprising given that *env* is generally under greater evolutionary pressure as it is responsible for the virus binding to the host cells [49]. All loci under diversifying selection were detected in the

FIV *pol* integrase region. Putting these lines of evidence together, we not only detected population-level impacts of demographic changes due to cessation of hunting on viral mutation, but also at the individual scale with stronger evolutionary pressure on viruses infecting males. Increased evolutionary pressure on the virus may increase the probability of a new FIV_{pco} phenotype occurring in this population. Systematic shifts in evolutionary pressure are known to occur when viruses switch hosts [e.g., 50,51]; however here we show that selective constraints on a virus can be altered in response to host demographic changes caused by wildlife hunting. We stress that FIV_{pco} is largely apathogenic in puma and therefore our findings demonstrate the types of changes in pathogen transmission dynamics that can be caused by hunting induced changes in wildlife populations.

Perturbation, management and disease

Our work provides a valuable case study on how changing hunting pressure can have unexpected consequences for pathogen transmission and evolution across scales. Our analytical approach was particularly valuable in helping deconstruct how shifts in population structure imprint on pathogen dynamics and evolution. For example, previous work using landscape genetic models only detected weak or inconsistent sex effects shaping FIV spread [34,39,52]. Our transmission network and phylodynamic approach, in contrast, was able to clearly distinguish the role of males in putative transmission chains and in accruing genetic diversity even though the data requirements are similar (e.g., a time scaled phylogeny). Scale dependence may be one reason for the difference as landscape genetics approaches obscure individual transmission events while quantifying the population-level signature of host and landscape on pathogen spread [53]. The putative transmission events we detected, supported by observational data, provided important

mechanistic details at an individual scale that enabled us tease out the links between management, sex and transmission that are difficult to detect otherwise. The shift in connectivity for each sex within the observed transmission network between sexes provided context to the differences in pathogen evolution we detected between the no-hunting and hunting periods. Our study provides new dimensions to the importance of understanding sex-specific variation when managing infectious disease in wildlife [e.g., 17,54]. We stress that our findings are specific to FIV in puma but also note that there is growing evidence that chronic lifelong retroviral infections, such as FIV, may be a useful apathogenic proxy for other directly transmitted and more virulent pathogens [38,55].

Our results provide a case study of the complex interplay between wildlife management and demography in shaping pathogen dynamics. In our case the cessation of hunting in a region facilitated demographic change via increased male survivorship and abundance [24], with potential increases in male-to-male contact behavior. Even though the 'perturbation' was the *cessation* of hunting, the underlying mechanism could be similar (e.g., lead to demographic and behavioural shifts that increase transmission). An expansion in the way we think about perturbations to include a cessation of a practice leading to demographic or behavioral change may be warranted. Any period of perturbation (intended or otherwise) to the demographic structure of a wildlife population for which disease poses a significant threat (e.g., the Florida panther [33], Tasmanian devils [12]) may warrant additional pathogen surveillance and potential disease mitigation plans.

Our results also reveal potential shortcomings of relying on population estimates of prevalence to understand the impact of wildlife management actions on pathogen transmission. In our case,

population estimates of FIV_{pco} prevalence across time alone could not detect shifts in transmission associated with hunting and were not sensitive to changes in population size (Figs. S8/S9). The lack of signal from prevalence data may be a contributing factor behind the variability of the effects of hunting on disease dynamics in empirical systems. Prevalence data may be better able to detect shifts in population demography where the pathogen causes acute infections with shorter periods of immunity.

The collection of pathogen molecular data from well-sampled wildlife populations across time is a logistical challenge, yet with ever cheaper and more mobile sequencing platforms, the potential to use approaches similar to ours is increasing, even for slowly evolving pathogens such as bacteria [25]. Our multidisciplinary approach can not only provide novel insights into the broader consequences of wildlife management on disease dynamics but can also help understand evolutionary relationships between hosts and pathogens in free-ranging species more broadly.

Materials and Methods

Study area and puma capture

Our study was conducted in two regions in the Rocky Mountains in Colorado separated by ~500 km but at similar elevations and with similar estimates of puma abundance [24,56], vegetative and landscape attributes, yet with differing degrees of urbanization (see Fig. S10 and [57]). In the treatment region in the Uncompahgre Plateau on the Western Slope of Colorado, blood samples were taken from 114 individuals (Table S1) and monitored intensively (i.e., very high frequency radio and GPS collars) until their death or the end of the study in 2014. In the stable management

region in the Front Range of Colorado, blood samples were taken from 56 individuals from 2005-2014. Captured pumas were anesthetized with established sedative and tranquilizer protocols [24] and released after blood, serum, and oral swabs were collected. Animal sex, age, and capture location were recorded. See [39] for sample storage, FIV_{pco} DNA extraction and sequencing details. In brief, for samples that were qPCR positive for FIV_{pco}, the complete *ORFA* and *pol* gene regions were isolated using a nested PCR protocol [39]. Recombination was removed and the genes were concatenated together. See Tables S1 and S2 for a summary of the sequence data and a comparison of study area size, estimates of host abundances, host mortality, and host genetic diversity between regions.

Transmission and phylogenetic trees

We constructed transmission trees between pumas in each region using the R package *TransPhylo* [22]. *TransPhylo* uses a time-stamped phylogeny to estimate a transmission tree to gain inference into "who infected whom" and when. Briefly, this approach computes the probability of an observed transmission tree given a phylogeny using a stochastic branching process epidemiological model; the space of possible transmission trees is sampled using reversible jump Markov chain Monte Carlo (MCMC) [22]. This approach is particularly useful for pathogens where the outbreak is ongoing, and not all cases are sampled [22], as is the case here. We leveraged our FIV_{pco} Bayesian phylogenetic reconstructions from previous work and focused on the two clades of FIV_{pco} that predominantly occurred in each region (see [39]). Whilst the *TransPhylo* approach makes few assumptions, a generation time distribution (the time from primary infection to onward transmission) is required to calibrate the epidemiological model [22]. We assumed that generation time could be drawn from a Gamma distribution ($k = 2$, $\theta = 1.5$) estimating onward transmission on average 3 years post-infection (95% interval: 0.3 - 8 years, based on average

353 puma age estimates [44]). Based on previous work [24,57] (see Table S1 for treatment region
354 estimates), we were confident that the proportion of cases (π) sampled was high, therefore we set
355 the starting estimate of π to be 0.6 (60% of cases tested in each region), and allowed it to be
356 estimated by the model. We ran multiple MCMC analyses of 400,000 iterations and assessed
357 convergence by checking that the parameter effective sample size (ESS) was > 200. We
358 computed the posterior distributions of R_0, π, and the realized generation time from the MCMC
359 output. We also estimated likely infection time distributions for each individual and compared
360 these estimates to approximate puma birth dates to ensure that these infection time distributions
361 were biologically plausible. We then computed a consensus transmission tree for each region to
362 visualize the transmission probabilities between individuals through time. Lastly, we reformatted
363 the tree into a network object (nodes as individual puma and edges representing transmission
364 probabilities) and plotted it using the *igraph* package [58] and overlaid puma sex as a trait. Overall
365 weighted degree and weighted degree for each sex, including edges representing homophily
366 (e.g., male-male) and heterophily (e.g., male-female), were also calculated using *igraph*. See [59]
367 for more details on the *TransPhylo* pipeline.

368 To test the sensitivity of our results, we reconstructed transmission trees using the *TransPhylo*
369 approach above but randomly dropping a tip from each FIV_{pco} phylogeny in each region. As
370 running this transmission tree approach is computationally demanding, we performed ten
371 iterations and summarised our estimates of R_0 and weighted degree homophily.

372 *Simulation modelling*

373 To test for non-random patterns of weighted degree between each sex, we applied a simulated
374 network annealing approach from the *Ergm* R package (Handcock et al, 2018). To generate each
375 simulated network, we fitted a variety of probability distributions to edge weight and degree of

the transmission networks in both treatment and stable regions, then used AIC to select the best fitting target distribution. We were unable to subdivide the treatment region into hunting and no-hunting periods as there were no transmission events detected to help parametrize the models after 2012. Edge density, network size and the number of isolated nodes were fixed based on each observed network. We added sex to each simulated node attribute drawing from a Bernoulli distribution (probability= 0.5). Using these network characteristics, we generated 1000 'null' networks and compared the homophily weighted degree distribution of each sex (i.e., the average weighted degree for each individual based on putative male-male or female-to-female transmission events) of the null networks to the observed and calculated a bootstrap p-value.

Selection analyses

To test if the demographic changes driven by hunting resulted in a reduction in the intensity of natural selection on FIV_{pco}, we examined selective pressure in both time periods in each region using the RELAX hypothesis testing framework [60]. The method builds upon random effects branch-site models (BS-REL) [61] that estimates the ω ratio (the ratio of non-synonymous to synonymous mutations or dN/dS) along each branch from a discrete distribution of three ω ratio classes allowing selection pressure to vary across the phylogeny [60]. A ω ratio of one corresponds to neutral selection with values > 1 being evidence for diversifying (positive) selection along a branch, and < 1 evidence for purifying (negative) selection along a branch. Briefly, RELAX tests for relaxation of selection pressure by dividing branches into three subsets; test branches (T), reference branches (R) and unclassified branches (U) [60] with ω_T (resp. ω_R) being the estimated dN/dS ratio on test (resp. reference) branches. The discrete distribution of ω is calculated using BS-REL for each branch class, and then branches belonging to each subset are compared. The reference estimates of ω are raised to the power of k (an intensity parameter) so that $\omega_T = \omega_R^k$ in

order to simplify model comparison. The null RELAX model is when the ω distribution and thus selective pressure is the same in R and T (when $k = 1$). The null model is compared to an alternate model (using a likelihood ratio test) that allows k to vary so that when $k > 1$ selection pressure on the test branches was intensified or $k < 1$ indicating that selection pressure has been relaxed [60]. In the relaxed scenario, $k < 1$ branches in R are under stronger purifying and diversifying selection compared to T branches (e.g., ω shifts from 0.1 to 0.001 or from 10 to 2). See [60] for model details. T and R were selected from leaf branches (all other branches were Unassigned, U); individuals sampled from 2005-2011 (to the end of the lag period) were assigned to the R set and those sampled from 2012-2014 were assigned to T set. All branches not directly connecting to the tips were classified as 'U' as the majority had low phylogenetic support (posterior probability < 0.6). To further interrogate the sequence data to identify individual sites under selection, we performed the MEME (mixed-effects model of evolution) pipeline [62]. For the putative sites under selection, we scanned the alignment to help determine which lineages/hosts accrued infections with these non-synonymous substitutions. We performed both MEME and RELAX models using the Datamonkey web application [63].

Population growth rate

We applied the non-parametric *skygrowth* method [47] to examine if the FIV_{Pco} population growth rate fluctuated across time and if this was related to changes in male or female population size in the treatment region. We did not relate puma population sizes to FIV_{Pco} growth rates for the stable region as similar host population size estimates through time were not available. We fitted these models using MCMC (100,000 iterations) assuming that FIV_{Pco} population size fluctuated every 6 months over a 14-year period (the estimated time to most recent common ancestor of this

clade, Fig. S7). Otherwise, the default settings were used. We then performed a Pearson correlation test to assess if the trend in FIV_{Pco} population growth was related to male and female population size estimates [24]. Measuring the correlation between population size estimates and patterns of population growth using generalized linear models [47,64] was not feasible due to the relatively small size of this dataset.

Phylogenetic diversity

To quantify phylogenetic diversity in each time period in each region, we calculated the standardized effect size (SES) for Faith's phylogenetic richness that accounts for differing sample sizes (SES for Faith's PD, [65]). Faith's PD (hereafter PD) is the sum of the branch lengths of the phylogenetic tree linking all isolates for each subset (in this case the two time periods). As the number of isolates in each contrast differed (stable region 2005-2011: 11 isolates, stable region 2012-13: 5 isolates, treatment region 2005-2011: 10 isolates, treatment region 2012-14: 5 isolates) we calculated the standardized effect size (SES) by comparing the PD we observed to a null model that accounts for number of tips (i.e., how much phylogenetic diversity would we see for a given number of isolates by chance). We denote the standardized PD as SES.PD from here on; this was calculated across a subset of posterior phylogenetic trees from our previous Bayesian phylogenetic analyses [39]. To capture phylogenetic uncertainty in these estimates, we utilized the computational efficiency of the *PhyloMeasures* R package algorithm [66] to calculate SES.PD and apply this across a 1000 tree subsample of posterior trees [39]. Specifically, for each calculation of SES.PD we compared our observed PD to a uniform null model (i.e., isolate samples are taken with equal [uniform] probability). The code and data to perform these operations as well as the transmission tree analysis above can be found here: https://github.com/nfj1380/TransmissionDynamics_HuntingPuma

References:

1. Packer, C. *et al.* Sport hunting, predator control and conservation of large carnivores. *PLoS ONE* **4**, (2009).
2. Whitman, K., Starfield, A. M., Quadling, H. S. & Packer, C. Sustainable trophy hunting of African lions. *Nature* **428**, 175–178 (2004).
3. Treves, A. Hunting for large carnivore conservation. *Journal of Applied Ecology* vol. 46 1350–1356 (2009).
4. Milner-Gulland, E. J. *et al.* Reproductive collapse in saiga antelope harems. *Nature* **422**, 135 (2003).
5. Bischof, R. *et al.* Implementation uncertainty when using recreational hunting to manage carnivores. *J. Appl. Ecol.* **49**, 824–832 (2012).
6. Booth, V. R., Masonde, J., Simukonda, C. & Cumming, D. H. M. Managing hunting quotas of African lions (Panthera leo): A case study from Zambia. *J. Nat. Conserv.* **55**, 125817 (2020).
7. Potapov, A., Merrill, E. & Lewis, M. A. Wildlife disease elimination and density dependence. *Proc. R. Soc. B Biol. Sci.* **279**, 3139–3145 (2012).
8. Lloyd-Smith, J. O. *et al.* Should we expect population thresholds for wildlife disease? *Trends in Ecology and Evolution* vol. 20 511–519 (2005).
9. Choisy, M. & Rohani, P. Harvesting can increase severity of wildlife disease epidemics. *Proc. R. Soc. B Biol. Sci.* **273**, 2025–2034 (2006).
10. Beeton, N. & McCallum, H. Models predict that culling is not a feasible strategy to prevent extinction of Tasmanian devils from facial tumour disease. *J. Appl. Ecol.* **48**, 1315–1323 (2011).
11. Allendorf, F. W. & Hard, J. J. Human-induced evolution caused by unnatural selection through harvest of wild animals. *Proc. Natl. Acad. Sci.* **106**, 9987 LP – 9994 (2009).

12. Hamede, R. K., Bashford, J., McCallum, H. & Jones, M. Contact networks in a wild Tasmanian devil (*Sarcophilus harrisii*) population: using social network analysis to reveal seasonal variability in social behaviour and its implications for transmission of devil facial tumour disease. *Ecol. Lett.* **12**, 1147–1157 (2009).
13. Woodroffe, R. *et al.* Culling and cattle controls influence tuberculosis risk for badgers. *Proc. Natl. Acad. Sci. U. S. A.* **103**, 14713–14717 (2006).
14. Carr, A. N. *et al.* Wildlife management practices associated with pathogen exposure in non-native wild pigs in Florida, U.S. *Viruses* **11**, (2019).
15. Woodroffe, R., Cleaveland, S., Courtenay, O., Laurenson, M. K. & Artois, M. Infectious disease in the management and conservation of wild canids. in *The Biology and Conservation of Wild Canids* 123–142 (Oxford University Press, 2004). doi:10.1093/acprof:oso/9780198515562.003.0006.
16. Carter, S. P. *et al.* Culling-induced social perturbation in Eurasian badgers *Meles meles* and the management of TB in cattle: An analysis of a critical problem in applied ecology. *Proc. R. Soc. B Biol. Sci.* **274**, 2769–2777 (2007).
17. Silk, M. J. *et al.* Contact networks structured by sex underpin sex-specific epidemiology of infection. *Ecol. Lett.* **21**, 309–318 (2018).
18. Silk, M. J. *et al.* The application of statistical network models in disease research. (2017) doi:10.1111/2041-210X.12770.
19. Morters, M. K. *et al.* Evidence-based control of canine rabies: a critical review of population density reduction. *J. Anim. Ecol.* **82**, 6–14 (2013).
20. Lachish, S., McCallum, H., Mann, D., Pukk, C. E. & Jones, M. E. Evaluation of selective culling of infected individuals to control tasmanian devil facial tumor disease. *Conserv. Biol. J. Soc. Conserv. Biol.* **24**, 841–51 (2010).

21. Grubaugh, N. D. *et al.* Tracking virus outbreaks in the twenty-first century. *Nature Microbiology* vol. 4 10–19 (2019).
22. Didelot, X., Fraser, C., Gardy, J. & Colijn, C. Genomic infectious disease epidemiology in partially sampled and ongoing outbreaks. *Mol. Biol. Evol.* **34**, msw075 (2017).
23. Smith, M. D. *et al.* Less is more: An adaptive branch-site random effects model for efficient detection of episodic diversifying selection. *Mol. Biol. Evol.* **32**, 1342–1353 (2015).
24. Logan, K. A. & Runge, J. P. Effects of hunting on a puma population in Colorado. *Wildl. Monogr.* 1–35 (2020).
25. Biek, R., Pybus, O. G., Lloyd-Smith, J. O. & Didelot, X. Measurably evolving pathogens in the genomic era. *Trends in Ecology and Evolution* vol. 30 306–313 (2015).
26. Pybus, O. G., Tatem, A. J. & Lemey, P. Virus evolution and transmission in an ever more connected world. *Proceedings of the Royal Society B: Biological Sciences* vol. 282 (2015).
27. Woolhouse, M. E. J., Adair, K. & Brierley, L. RNA viruses: A case study of the biology of emerging infectious diseases. in *One Health* 83–97 (American Society of Microbiology, 2014). doi:10.1128/microbiolspec.oh-0001-2012.
28. Pybus, O. G. & Rambaut, A. Evolutionary analysis of the dynamics of viral infectious disease. *Nature Reviews Genetics* vol. 10 540–550 (2009).
29. Fountain-Jones, N. M. *et al.* Towards an eco-phylogenetic framework for infectious disease ecology. *Biol. Rev.* **93**, 950–970 (2018).
30. Webb, C. O. Exploring the phylogenetic structure of ecological communities: An example for rain forest trees. *Am. Nat.* **156**, 145–155 (2000).
31. Biek, R. *et al.* Epidemiology, genetic diversity, and evolution of endemic feline immunodeficiency virus in a population of wild cougars. *J. Virol.* **77**, 9578–9589 (2003).

32. Pedersen, N. C., Yamamoto, J. K., Ishida, T. & Hansen, H. Feline immunodeficiency virus infection. *Vet. Immunol. Immunopathol.* **21**, 111–129 (1989).
33. Malmberg, J. L. *et al.* Altered lentiviral infection dynamics follow genetic rescue of the Florida panther. *Proc. R. Soc. B Biol. Sci.* **286**, 20191689 (2019).
34. Fountain-Jones, N. M. *et al.* Linking social and spatial networks to viral community phylogenetics reveals subtype-specific transmission dynamics in African lions. *J. Anim. Ecol.* **86**, 1469–1482 (2017).
35. Elbroch, L. M., Levy, M., Lubell, M., Quigley, H. & Caragiulo, A. Adaptive social strategies in a solitary carnivore. *Sci. Adv.* **3**, e1701218 (2017).
36. Sweanor, L. L., Logan, K. A. & Hornocker, M. G. Cougar dispersal patterns, metapopulation dynamics, and conservation. *Conserv. Biol.* **14**, 798–808 (2000).
37. Gehrt, S. D., Riley, S. P. D. & Cypher, B. L. *Urban carnivores : ecology, conflict, and conservation*. (Johns Hopkins University Press, 2010).
38. Gilbertson, M. L. J. *et al.* Transmission of one predicts another: Apathogenic proxies for transmission dynamics of a fatal virus. *bioRxiv* 2021.01.09.426055 (2021) doi:10.1101/2021.01.09.426055.
39. Fountain-Jones, N. M. *et al.* Host relatedness and landscape connectivity shape pathogen spread in a large secretive carnivore. *Commun. Biol.* **4**, (2021).
40. Hornocker, M. G. & Negri, Sharon. *Cougar : ecology and conservation*. (University of Chicago Press, 2010).
41. Moss, W. E., Alldredge, M. W. & Pauli, J. N. Quantifying risk and resource use for a large carnivore in an expanding urban-wildland interface. *J. Appl. Ecol.* **53**, 371–378 (2016).
42. Trumbo, D. *et al.* Urbanization impacts apex predator gene flow but not genetic diversity across an urban-rural divide. *Mol. Ecol.* **28**, 4926–4940 (2019).

546 43. VandeWoude, S. & Apetrei, C. Going wild: lessons from naturally occurring T-
547 lymphotropic lentiviruses. *Clin. Microbiol. Rev.* **19**, 728–762 (2006).
548 44. Logan, K. A. & Sweanor, L. L. *Desert puma : evolutionary ecology and conservation of*
549 *an enduring carnivore*. (Island Press, 2001).
550 45. Trumbo, D. *et al.* Urbanization impacts apex predator gene flow but not genetic diversity
551 across an urban-rural divide. *Mol. Ecol.* **28**, 4926–4940 (2019).
552 46. Krakoff, E., Gagne, R. B., VandeWoude, S. & Carver, S. Variation in Intra-individual
553 Lentiviral Evolution Rates: a Systematic Review of Human, Nonhuman Primate, and
554 Felid Species. *J. Virol.* **93**, e00538-19 (2019).
555 47. Volz, E. M. & Didelot, X. Modeling the growth and decline of pathogen effective
556 population size provides insight into epidemic dynamics and drivers of antimicrobial
557 resistance. *Syst. Biol.* **67**, 719–728 (2018).
558 48. Murrell, B. *et al.* Detecting individual sites subject to episodic diversifying selection.
559 *PLoS Genet.* **8**, (2012).
560 49. Kenyon, J. C. & Lever, A. M. L. The molecular biology of feline immunodeficiency
561 virus (FIV). *Viruses* vol. 3 2192–2213 (2011).
562 50. Tamuri, A. U., dos Reis, M., Hay, A. J. & Goldstein, R. A. Identifying Changes in
563 Selective Constraints: Host Shifts in Influenza. *PLoS Comput. Biol.* **5**, e1000564 (2009).
564 51. Forni, D., Cagliani, R., Clerici, M. & Sironi, M. Molecular Evolution of Human
565 Coronavirus Genomes. *Trends in Microbiology* vol. 25 35–48 (2017).
566 52. Fountain-Jones, N. M. *et al.* Urban landscapes can change virus gene flow and evolution
567 in a fragmentation-sensitive carnivore. *Mol. Ecol.* **26**, 6487–6498 (2017).
568 53. Kozakiewicz, C. P. *et al.* Pathogens in space: Advancing understanding of pathogen
569 dynamics and disease ecology through landscape genetics. *Evol. Appl.* (2018)
570 doi:10.1111/eva.12678.

54. McDonald, J. L., Smith, G. C., McDonald, R. A., Delahay, R. J. & Hodgson, D. Mortality trajectory analysis reveals the drivers of sex-specific epidemiology in natural wildlife–disease interactions. *Proc. R. Soc. B Biol. Sci.* **281**, 20140526 (2014).
55. Gilbertson, M. L. J., Fountain-Jones, N. M. & Craft, M. E. Incorporating genomic methods into contact networks to reveal new insights into animal behaviour and infectious disease dynamics. *Behaviour* **155**, 759–791 (2018).
56. Alldredge, M. W., Blecha, T. & Lewis, J. H. Less invasive monitoring of cougars in Colorado's front range. *Wildl. Soc. Bull.* **43**, 222–230 (2019).
57. Lewis, J. S. *et al.* The effects of urbanization on population density, occupancy, and detection probability of wild felids. *Ecol. Appl.* **25**, 1880–1895 (2015).
58. Csárdi, G. & Nepusz, T. The igraph software package for complex network research. *InterJournal Complex Syst.* 1695 (2006).
59. Didelot, X., Kendall, M., Xu, Y., White, P. J. & McCarthy, N. Genomic Epidemiology Analysis of Infectious Disease Outbreaks Using TransPhylo. *Curr. Protoc.* **1**, e60 (2021).
60. Wertheim, J. O., Murrell, B., Smith, M. D., Pond, S. L. K. & Scheffler, K. RELAX: Detecting relaxed selection in a phylogenetic framework. *Mol. Biol. Evol.* **32**, 820–832 (2015).
61. Kosakovsky Pond, S. L. *et al.* A random effects branch-site model for detecting episodic diversifying selection. *Mol. Biol. Evol.* **28**, 3033–3043 (2011).
62. Murrell, B. *et al.* Detecting individual sites subject to episodic diversifying selection. *PLoS Genet.* **8**, (2012).
63. Weaver, S. *et al.* Datamonkey 2.0: A modern web application for characterizing selective and other evolutionary processes. *Mol. Biol. Evol.* **35**, 773–777 (2018).

64. Gill, M. S., Lemey, P., Bennett, S. N., Biek, R. & Suchard, M. A. Understanding past population dynamics: Bayesian coalescent-based modeling with covariates. *Syst. Biol.* **65**, 1041–1056 (2016).
65. Faith, D. P. Conservation evaluation and phylogenetic diversity. *Biol. Conserv.* **61**, 1–10 (1992).
66. Tsirogiannis, C. & Sandel, B. PhyloMeasures: a package for computing phylogenetic biodiversity measures and their statistical moments. *Ecography* **39**, 709–714 (2016).
67. Fountain-Jones, N. *et al.* Emerging phylogenetic structure of the SARS-CoV-2 pandemic. *Virus Evol.* **6**, 2020.05.19.103846 (2020).
68. Karcher, M. D., Palacios, J. A., Bedford, T., Suchard, M. A. & Minin, V. N. Quantifying and mitigating the effect of preferential sampling on phylodynamic inference. *PLOS Comput. Biol.* **12**, e1004789 (2016).

607

608 **Box 1.** Description of key social network, transmission tracing and phylodynamic
609 terminology used in the manuscript.

Term	Definition
R_0	The basic reproduction number 'R naught' is the expected number of cases generated by one case in a population of susceptible individuals.
Transmission bottleneck	Transmission of viruses between hosts usually involves a relatively small number of virus particles being exchanged between hosts (e.g., [53]). This has the effect of reducing viral genetic diversity population size and creating a 'bottleneck'.
Purifying selection	'Negative selection' is the removal of nonsynonymous mutations (i.e., mutations that lead to a change in protein coding).
Diversifying selection	'Positive selection' is the favoring of nonsynonymous mutations that yield an adaptive advantage. These mutations can rapidly increase in frequency across a population.
Transmission network	A network where nodes represent individual puma and edges reflect transmission events based on transmission tree estimates. Edge weights are the probability of the transmission event occurring. Transmission trees generated by the R package 'TransPhylo' (Didelot et al, 2017) estimate who infected whom, including potentially unsampled individuals using a stochastic branching epidemiological model and a time-scaled phylogeny.
Weighted degree	The summed probability of a individual puma (i.e., a node in the network) being involved in transmission events divided by the number of transmission events (i.e., edges in the network).
Weighted degree homophily	The weighted degree of transmission events between members of the same sex.
Skygrowth demographic analyses	Non-parametric population- genetic model estimating the growth effective population size through time (a surrogate for genetic diversity) using Bayesian inference. This method has been shown to accurately reconstruct pathogen outbreak dynamics in a variety of systems ([47,67]).

610

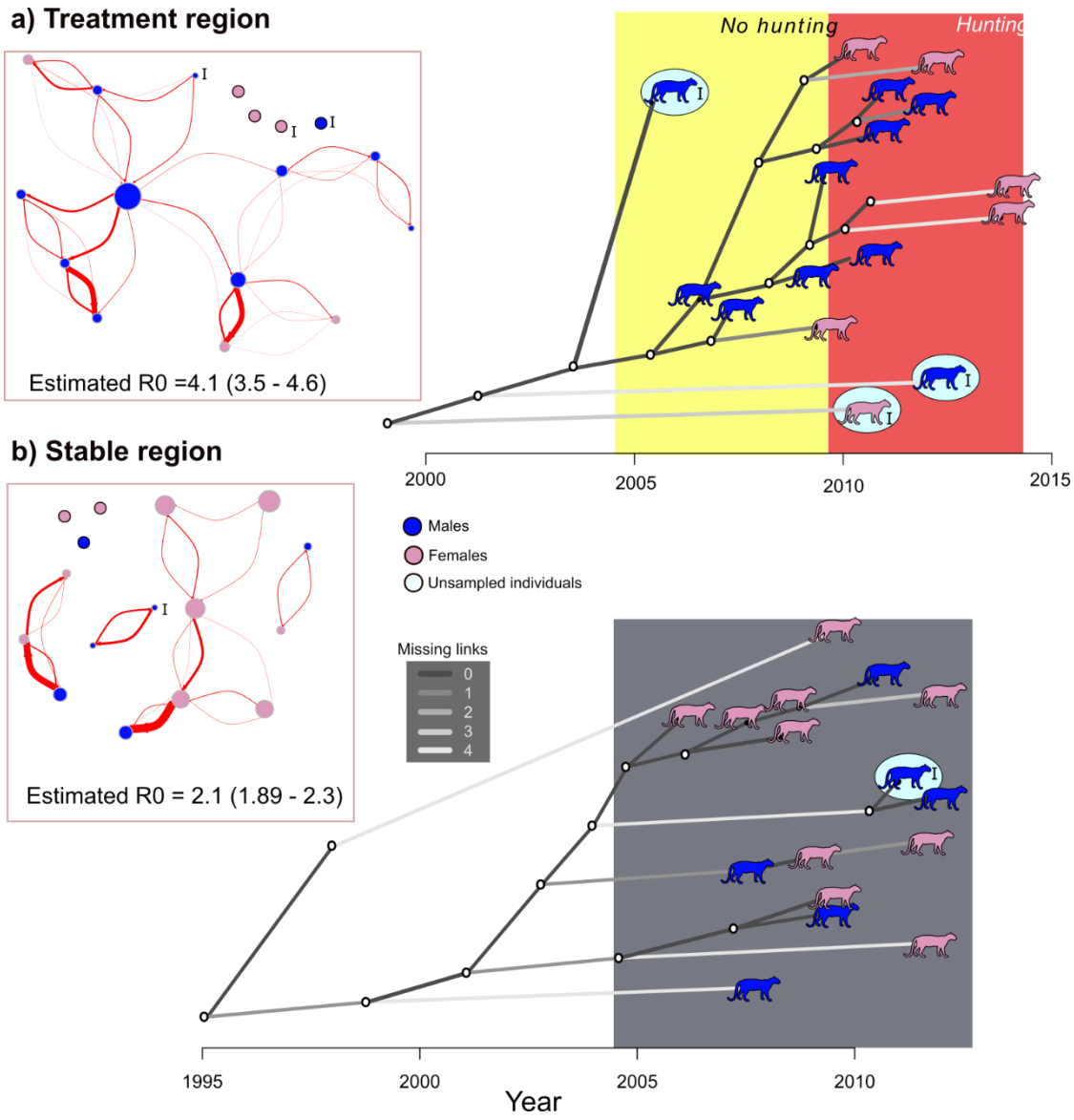

Fig. 1. Males (blue nodes/puma silhouettes) were dominant in the FIV_{pco} transmission network in the treatment region (a) whereas females (pink nodes/puma silhouettes) were more central in the transmission network in the stable region (b). Nodes connected to each other via edges indicate the probability of transmission in either direction. Node size in the networks (left) is scaled based on the number of edges estimated for each individual. Edge width is scaled according to the probability of the transmission events, where wider edges indicate a more likely transmission event (see Fig. S1). R_0 estimates (with 95% highest posterior density (HPD)) are based on the stochastic branching epidemiological model underlying each transmission network (see *Materials & Methods*, [22]). Transmission trees

(right) show these putative transmission events through time with branch color indicating how many missing edges are likely between individuals. Yellow: hunting pressure relieved; red: hunting pressure resumed; grey: stable region. White nodes: unsampled individuals estimate by the model. I: individuals that were likely immigrants in this region based on [45]. See Figure S2 for the FIV_{pco} generation time distributions for each region and Figure S3 for the estimate of missing cases across year

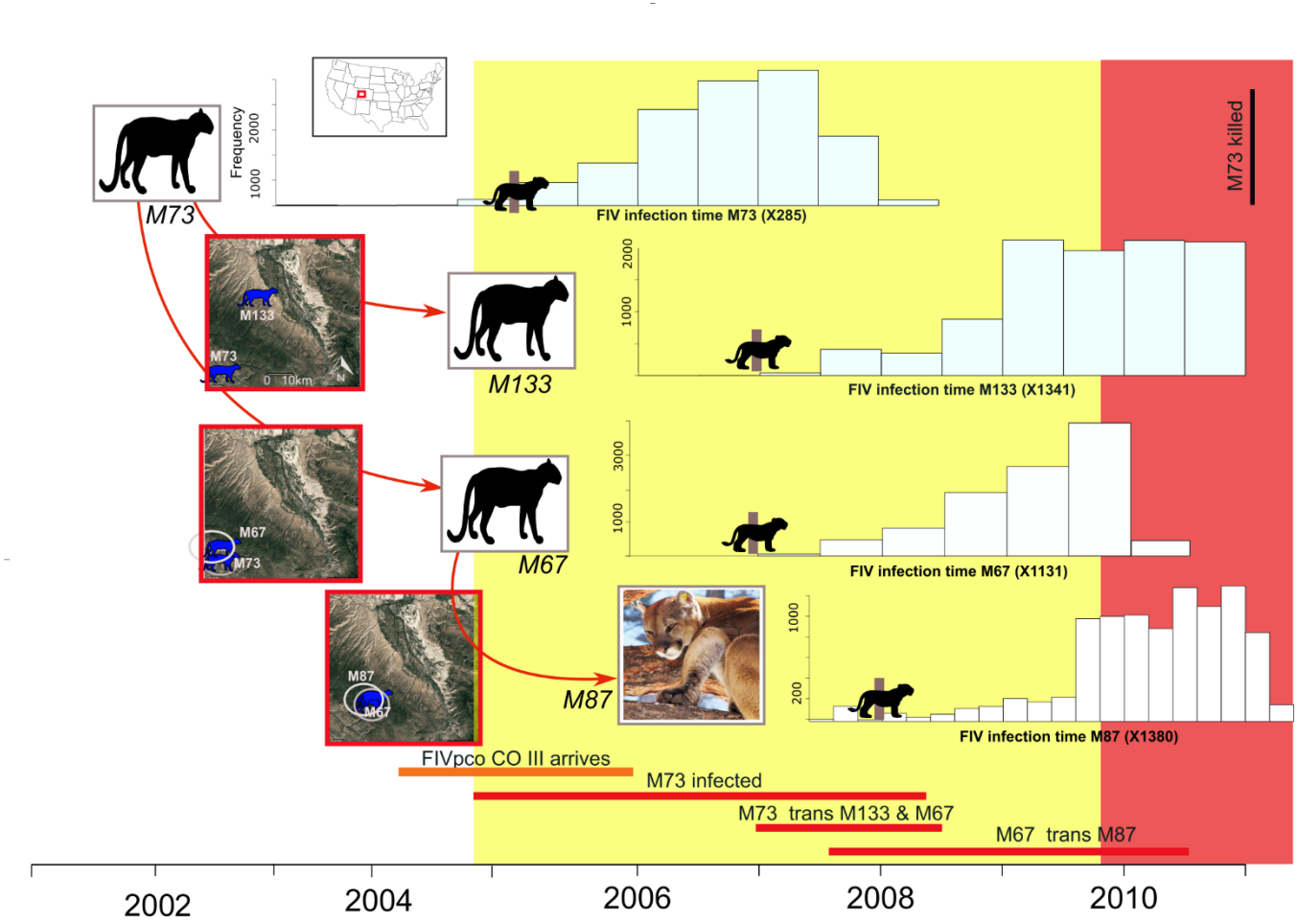

627

628 **Fig. 2:** Infection time distributions from our transmission network model for individuals involved in a putative transmission chain, along with

629 the likely direction of transmission (red arrows) and the spatial context (see Fig. S5/S6 for information on other transmission events in the

630 treatment and stable region). Grey circles encompassing puma silhouettes in the map insets represent known territorial overlap between
631 individuals (based on unpublished radiotelemetry location estimates from K. Logan) and is not representative of territory size. Light yellow:
632 hunting pressure relieved. Birth year is indicated by the cub silhouette, and death year of M73 is indicated by the black horizontal line. The
633 orange horizontal line indicates when the FIV_{pco} CO III lineage was introduced into this population based on node estimates from [39]. Red
634 horizontal lines indicate transmission time distributions (overlap between infection time distributions) and ‘trans’ means ‘likely transmitted to’.

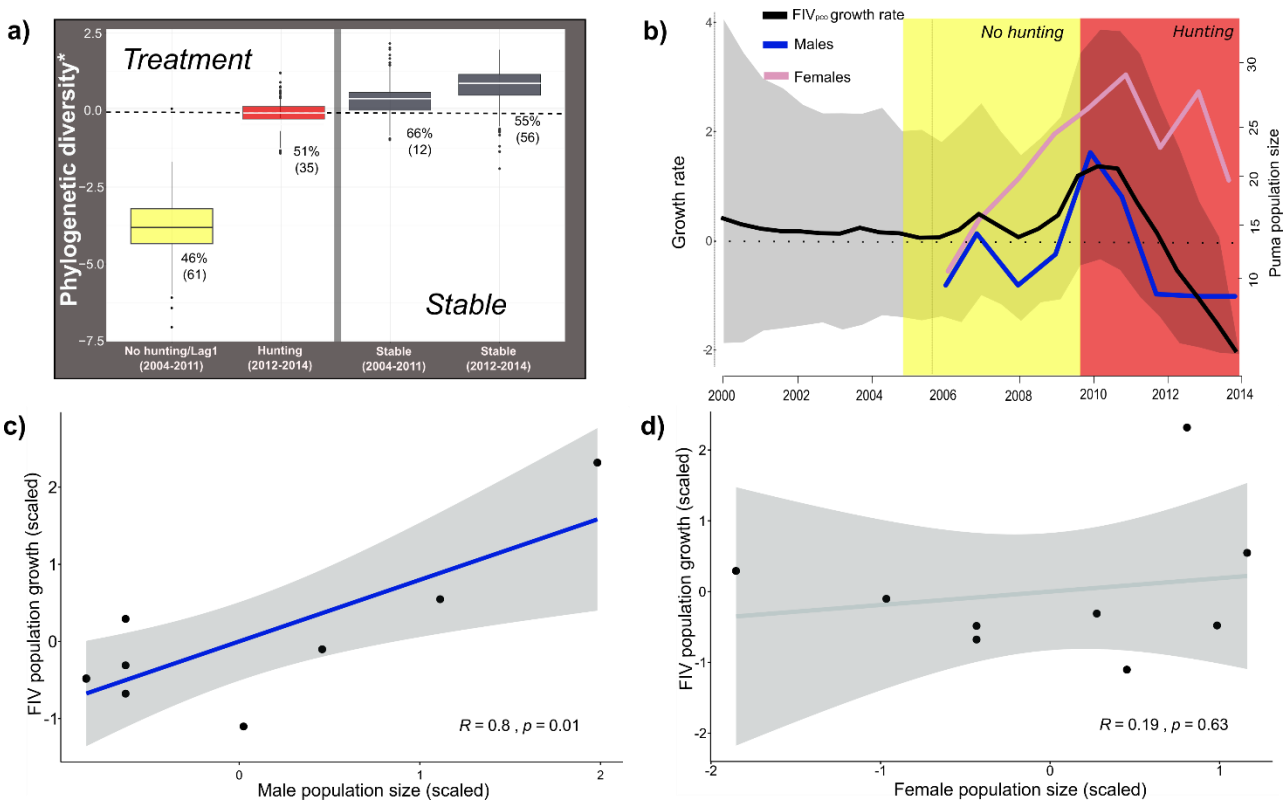

635

636 **Fig. 3.** Eliminating hunting mortality led to: (a) overall greater phylogenetic clustering (i.e.,
637 lower phylogenetic diversity) of FIV_{pco} isolates standardized for sample number and (b) an
638 increase in FIV_{pco} population growth rate that was (c) strongly correlated with male
639 population size rather than (d) female population size in the treatment region. (a)
640 Standardized phylogenetic diversity (*: SES.PD, standardized effect size phylogenetic
641 diversity calculated from 1000 posterior trees) estimates revealed strong patterns of
642 phylogenetic clustering (smaller distances between isolates than expected by chance) when
643 hunting pressure was relieved (negative values of SES.PD). Otherwise, FIV_{pco} isolates were
644 more dispersed across the tree (SES. PD ~ 0, indicated by the dashed line). Estimates of
645 FIV_{pco} prevalence (number of qPCR positives/total number sampled) are provided next to
646 each box and whisker plot with number of individuals tested shown in parentheses (see Fig.
647 S8 for estimates of prevalence across years). Sequences from puma sampled in the lag 2
648 period were included in the no-hunting period. There was only one sequence sampled in the
649 lag 1 period and this was retained in the hunting period as it made no difference to the

650 diversity estimate. (b) Viral population growth rate was estimated using Bayesian
651 phylodynamic reconstruction [47]. The dashed horizontal line reflects the 0-growth line. See
652 Fig. S7a for the corresponding skyline plot (effective population size through time estimated
653 via the *phylodyn* model [68]) for the treatment region and Fig. S7b/c for complementary plots
654 for the FIV_{pco} clade dominant in the stable region.

655

656

Acknowledgments: This project was funded by the National Science Foundation Ecology of Infectious Diseases research program grants (DEB 1413925) and an Australian Research Council Discovery Project Grant (DP190102020). M.L.J.G. was supported by the Office of the Director, National Institutes of Health under award number NIH T32OD010993. The content is solely the responsibility of the authors and does not necessarily represent the official views of the National Institutes of Health. SD is supported by the *Fonds National de la Recherche Scientifique* (FNRS, Belgium). GB acknowledges support from the Interne Fondsen KU Leuven / Internal Funds KU Leuven under grant agreement C14/18/094, and the Research Foundation – Flanders ('Fonds voor Wetenschappelijk Onderzoek – Vlaanderen', G0E1420N). MEC was funded by the National Science Foundation (DEB-1654609 and 2030509) and the CVM Research Office UMN Ag Experiment Station General Ag Research Funds. Any use of trade, firm, or product names is for descriptive purposes only and does not imply endorsement by the U.S. Government.

Data accessibility:

DNA sequences—GenBank accession: MN563193 - MN563239. All other data and code to perform the analysis are available on Github:

https://github.com/nfj1380/TransmissionDynamics_HuntingPuma